Physica Scripta. T92, 122–125, 2001

Systematic Study of Visible Transitions in Ti-like High Z Ions

H. Watanabe[1]*, F. J. Currell[2], T. Fukami[3], D. Kato[1], S. Ohtani[1,3] and C. Yamada[1,3]

[1]Cold Trapped Ions Project, ICORP, Japan Science and Technology Corporation (JST), Tokyo 182-0024, Japan
[2]The Queen's University of Belfast, Belfast, BT7 1NN, UK
[3]University of Electro-communications, Tokyo 182-8585, Japan

Received July 31, 2000; accepted September 26, 2000

PACS Ref: 32.30.Jc, 32.10.Fn, 31.15.Ar, 52.70.-m

Abstract

The magnetic dipole transitions between fine structure levels in the ground term of Ti-like ions, $(3d^4)\ ^5D_2-^5D_3$, were investigated by observation of visible and near-UV light for several elements with atomic numbers from 51 to 78. The wavelengths are compared with theoretical values we recently calculated. The differences between the present calculations and measurements are less than 0.6%. The anomalous wavelength stability predicted by Feldman, Indelicato and Sugar [J. Opt. Soc. Am. B **8**, 3 (1991)] was observed. We attribute this anomalous wavelength stability to the transition from *LS* to *JJ* coupling and the asymptotic behavior of the transition energies in the intermediate coupling regime.

1. Introduction

Visible lines have been observed in the solar corona. These lines were identified as forbidden lines from highly charged ions [1]. Lines from highly charged ions have also been observed in fusion plasmas and used for plasma diagnostics to obtain, for instance, ion temperature, density distribution and magnetic field distribution [2–4]. Hence, the measurement of forbidden lines from highly charged ions is important. Feldman, Indelicato and Sugar [5] performed multiconfiguration Dirac-Fock (MCDF) calculations to search for visible lines for diagnostics of high temperature plasmas. Their calculations predict that the wavelengths of the M1 transition between the fine structure levels in the ground term of Ti-like ions, $(3d^4)\ ^5D_2-^5D_3$, have almost the same value for elements with atomic numbers between $Z = 50$ and $Z = 92$. This behavior is rather anomalous, because usually the wavelength due to a specific transition decreases rapidly with increasing Z (almost proportional to Z^{-4}). This anomalous stability has drawn the attention of many researchers experimentally and theoretically. For Ti-like Xe, Ba Nd, Gd, Yb, W, Au and Bi ions, this transition has been measured at NIST [6–8], Oxford [9] and Lawrence Livermore National Laboratory (LLNL) [10,11] with electron beam ion traps (EBITs). The measured values have been used to verify the accuracy of theoretical results. In the early work by Feldman, Indelicato and Sugar [5] the differences were about 5%. More recent calculations performed by Beck [12,13], reduced those differences to less than 2% for Xe, Ba, Gd, Nd, W and Bi. For W and Bi [13] the errors were about 0.7% and 0.06%, respectively. The accuracy of his calculations was good, although the wavelengths were available only for those particular elements.

In this study the wavelengths of the $(3d^4)\ ^5D_2-^5D_3$ transition in Ti-like Sb, I, Xe, Cs, Ba, Sm, Eu, Hf, Ta, W, Re and Pt ions were measured and also those of the $(3d^4)\ ^5D_4-^5D_3$ transition were measured for Sm and Eu, simultaneously with the $(3d^4)\ ^5D_2-^5D_3$ transition. These values were compared with the theoretical values obtained by MCDF calculations. The anomalous wavelength variation predicted by Feldman, Indelicato and Sugar [5] is discussed based on the present calculations.

2. Experimental set-up

In this study, ions were produced with the Tokyo-EBIT at the University of Electro-Communications [14]. The electron beam was accelerated electrostatically and compressed by the magnetic field produced by superconducting magnets. The trap consisted of three coaxial cylindrical drift tubes, in which ions were trapped radially by the space-charge potential produced by the electron beam and axially by the potential applied to the end drift tubes relative to the center one. The ions were exposed to electron impact and hence were ionized successively, becoming highly charged ions. The conditions used for studying the various ions is shown in Table I.

Source ions were introduced into the trap using various methods. The EBIT was equipped with a gas injector to feed source elements or coolant gas into the trap. $Sb(CH_3)_3$, I_2 and Xe were introduced through the injector. Cs was injected from the top of the EBIT with a Cs ion source, Heat Wave Aluminosilicate Ion Source. Ba naturally evaporated from the cathode of the electron gun which was used as a source. The other elements were injected from the trap of the EBIT with a metal vapor vacuum arc (MEVVA) ion source.

The light emitted from the center of the trap was focused onto the entrance slit of a monochromator with a biconvex fused silica lens situated just outside the EBIT at 347 mm from the beam axis. The focal length of the lens was 153.8 mm and the diameter 100 mm. The monochromator, Jovin-Yvon HR320, was a Czerny-Turner type with a focal length of 320 mm. This was placed so that the entrance slit was at 612 mm from the beam axis. The slit width was set to 100 μm for all measurements. A grating with 600 grooves/mm, blazed at 750 nm was used in second order for the I, Xe, Cs, Ba measurements and one with 1200 grooves/mm, blazed at 400 nm was used in first order for the others. The light was detected with a liquid nitrogen cooled charge coupled device detector, Princeton Instruments LN/CCD-1100-PB/VISAR. The raw data sets were obtained as two dimensional images at the focal plain of the monochromator. The signals in the images were added vertically, i.e. perpendicular to the dispersion direction, to obtain spectra.

*e-mail: watanabe@hci.jst.go.jp

Table I. *Summary of experimental conditions.*

Z	Energy (KeV)	Current (mA)
51(Sb)	1.9	30
53(I)	2.0	23
54(Xe)	2.2	28
55(Cs)	2.5	32
56(Ba)	2.5	32
62(Sm)	3.4	74
63(Eu)	3.5	60
72(Hf)	4.8	105
73(Ta)	5.1	126
74(W)	5.3	126
75(Re)	5.5	100
78(Pt)	6.2	126

The calibration emission lines of neutral He, Ne, Ar, Kr and Hg were measured by introducing light from a window opposite the monochromator. The light travelled across the trap region before entering the monochromator. The position of the light sources during calibration spectra was different from that in the measurements. Systematic errors were checked by measuring lines with a known wavelength. The wavelength of the lines, based on the present calibration, coincided with the values listed in the literature within the uncertainties. Therefore the difference of the source position caused negligible systematic error in the wavelength scale.

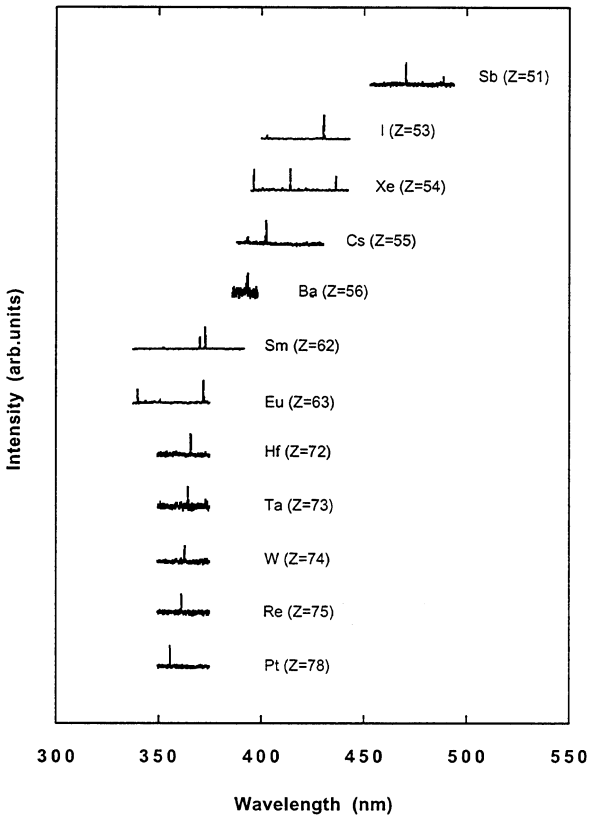

Fig. 1. The observed spectra of Ti-like Sb, I, Xe, Cs, Ba, Sm, Eu, Hf, Ta, W, Re and Pt ions. The vertical scales of the individual spectra have been adjusted so that the heights of the lines are almost the same.

3. Calculation

MCDF calculations have been performed using the GRASP92 code [15]. The Hamiltonian consisted of the one-particle Dirac Hamiltonian operator and the inter-electronic Coulomb interaction operator. The lowest order QED corrections except for the self-energy correction were included in the calculations. The nuclear charge distribution was approximated by the spherically symmetric Fermi model. In the case of highly charged ions, the contributions of higher excited states are considered to be small. The configuration space was divided into mutually orthogonal parts, P and Q. The P space was represented by a set of the reference configurations of $3d^4$, $3s^{-1}3d^5$, $3s^{-2}3d^6$ and $3p^{-2}3d^6$. The Q space was represented by the configurations of $3l^{-1}nl'$ $(4 \leq n \leq 7; l' \leq 6)$ and $3d^{-2}nln'l'$ $(4 \leq n, n' \leq 6; l, l, \leq 5)$. In the Hamiltonian matrix, the off-diagonal parts of the Q space were set to zero. This procedure resulted in a remarkable saving in CPU time, while it correctly included the contributions from Q space as a second order perturbation. The orbitals were optimized so that the sum of the energies of $J = 2$ and $J = 3$ was stationary with respect to a small change in the orbitals (Extended-Optimal-Level mode of the MCDF method). The details of the calculation will be presented elsewhere [16].

4. Results and Discussion

The obtained spectra are shown in Fig. 1. The wavelengths of the observed transitions are shown in Table II. The values in the parentheses are the uncertainties, which determined from the photon counting statistics and from the error in the wavelength scale.

These lines were identified with a combination of experimental and theoretical techniques. When the feed of the source elements was stopped, the lines disappeared, suggesting that they came from ions of the source elements. Moreover when the electron beam energy was set hundreds of eV above the energy at which Ti-like ions should be created, the lines began to appear and no other lines were observed in the region where the $(3d^4)\ {}^5D_2$–${}^5D_3$ and $(3d^4)\ {}^5D_4$–${}^5D_3$ transitions of Ti-like ions should be observed according to the theoretical predictions. Thus it is concluded that these lines were indeed due to the $(3d^4)\ {}^5D_2$–${}^5D_3$ or $(3d^4)\ {}^5D_4$–${}^5D_3$ transition of Ti-like ions.

In Fig. 2 the experimental wavelengths are shown together with the present theoretical values. The wavelengths of the $(3d^4)\ {}^5D_2$–${}^5D_3$ transition have been measured for several elements. For Xe, Ba and W, the wavelengths have been obtained by other groups [6,8–10]. These results coincide with the present ones within the range of the uncertainties except for the result of Ba reported by Bieber *et al.* [9]. When the present theoretical results are compared with the experimental wavelengths, the differences are less than 0.6% for all the elements. For elements above $Z = 60$ the differences are less than 0.16%, corresponding to about 0.5 nm in wavelength.

The anomalous behavior of the wavelength variation can be discussed based on the present theoretical calculations. In Fig. 3 the variation of the mixing coefficient is shown to show the change of the coupling scheme with respect

Table II. *Wavelengths of the* $(3d^4)\ ^5D_J–^5D_3$ $(J = 2, 4)$ *transition in Ti-like ions.*

	$(3d^4)\ ^5D_2–^5D_3$		$(3d^4)\ ^5D_4–^5D_3$	
Z	Measured (nm)	Calculated (nm)	Measured (nm)	Calculated (nm)
51(Sb)	470.24(3)[a]	472.77[a]		
53(I)	430.33(8)[a]	430.58[a], 410.95[h]		
54(Xe)	413.88(7)[a], 413.94(20)[b]	415.53[a], 395.25[h], 407.82[i]		
55(Cs)	402.14(11)[a]	402.73[a]		
56(Ba)	393.08(12)[a], 393.24(20)[b], 393.239(8)[c]	393.54[a], 386.53[i]		
60(Nd)	375.3(2)[d]	375.28[a], 355.68[h], 367.83[i]		
62(Sm)	372.52(3)[a]	372.28[a]	369.89(3)[a]	371.20[a]
63(Eu)	371.75(3)[a]	371.64[a]	339.48(4)[a]	340.94[a]
64(Gd)	371.3(2)[d]	371.10[a], 367.43[i]		
70(Yb)	367.64(15)[e]	367.57[a], 356.45[h]		
72(Hf)	365.54(4)[a]	365.33[a]		
73(Ta)	364.18(5)[a]	363.97[a]		
74(W)	362.67(5)[a], 362.6(2)[e], 362.713(10)[f]	362.47[a], 354.61[h], 360.50[j]		
75(Re)	361.06(5)[a]	360.81[a]		
78(Pt)	355.44(4)[a]	355.11[a]		
79(Au)	352.2(2)[g]	353.00[a]		
83(Bi)	344.29(15)[e]	343.77[a], 344.06[j]		

The numbers in parentheses are experimental uncertainties.
Wavelengths are values in air.
[a]This work.
[b]Morgan *et al.* [6].
[c]Bieber *et al.* [9].
[d]Serpa *et al.* [7].
[e]Porto *et al.* [8].
[f]Utter *et al.* [10].
[g]Träbert *et al.* [11].
[h]Feldman *et al.* [5].
[i]Beck [12].
[j]Beck [13].

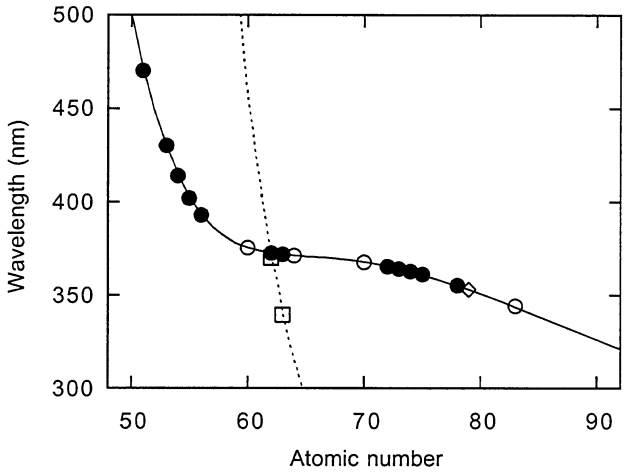

Fig. 2. The wavelengths of the $(3d^4)\ ^5D_2–^5D_3$ transition in Ti-like ions. ● are from our measurements. ○ are from the NIST group [6–8] and ◇ are from the LLNL group [11]. The solid line shows our theoretical wavelengths. The results of the $(3d^4)\ ^5D_4–^5D_3$ transition are also shown. □ are our experimental wavelengths. The dashed line shows our theoretical wavelengths. The results for Xe, Ba and W obtained by other groups [6,8–10] almost coincide with ours.

to Z, in which LS coupling states are taken as the basis. The mixing coefficients of the corresponding JJ coupling states are also shown. The levels which are well described by the LS coupling scheme in low Z region are characterized by the JJ coupling scheme in high Z region. It is clearly seen that the transition from LS to JJ coupling takes place in the relatively narrow region between $Z = 40$ and 60.

In Fig. 4 the transition energy between $J = 2$ and $J = 3$ levels is shown. The solid curve is the transition energy obtained with the intermediate coupling scheme. The dashed curve denotes ^5D component in the transition energy, while the dotted one denotes $3d_{3/2}{}^3 3d_{5/2}$ component. These curves form the asymptotes of the actual transition energy in the low and high Z regions, respectively. As shown in the figure, the behavior in the intermediate region interpolates between these asymptotic behaviors. In the case of the $J = 2 - 3$ transition, a plateau is formed accidentally due to the transition from LS to JJ coupling and also due to the asymptotic behaviors of the transition energies.

5. Conclusion

The wavelengths of the magnetic dipole transition between the fine structure levels in the ground term of Ti-like Sb, I, Xe, Cs, Ba, Sm, Eu, Hf, Ta, W, Re and Pt ions were measured in this study. The theoretical and experimental results agree well, with differences of less than 0.6% (2 nm) for all ions measured and less than 0.16% (0.5 nm) for the elements over $Z = 60$. The anomalous behavior predicted by Feldman, Indelicato and Sugar [5] was observed. It is concluded that the transition from the LS to the JJ coupling scheme and the asymptotic behavior of the transition energy are the reasons for the behavior.

Acknowledgements

This work was performed under the auspices of the International Cooperative Research Project (ICORP) of the Japan Science and Technology Corporation and partly supported by a Grant-in-Aid for Scientific Research (B-1048099) from the Ministry of Education, Science, Sports and Culture of Japan.

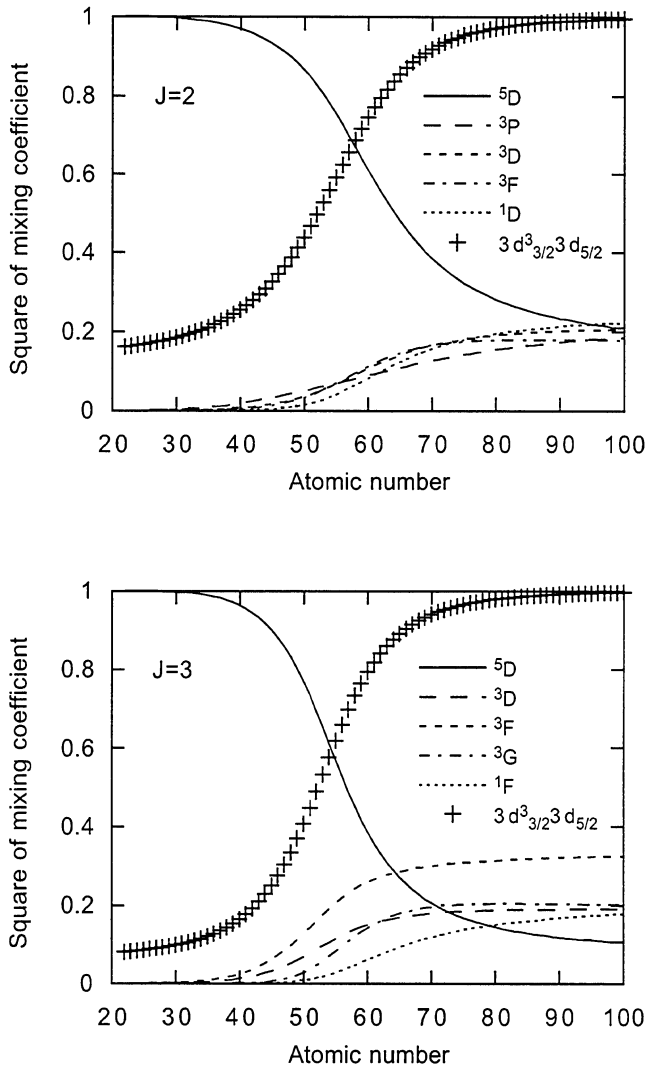

Fig. 3. The square of the mixing coefficient in the intermediate coupling scheme. The *LS* coupling states are taken as the basis. For information the square of the mixing coefficient is shown for the corresponding *JJ* coupling state taken as the basis.

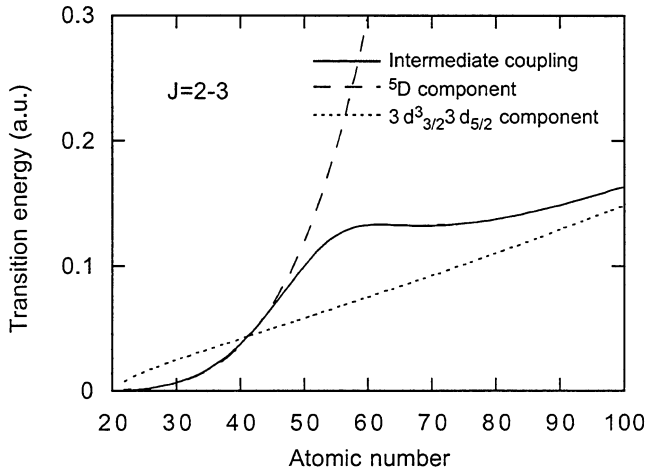

Fig. 4. The transition energy from $J = 3$ to $J = 2$ levels in the ground term of Ti-like ions. The dashed curve denotes ^{5}D component in the transition energy, while the dotted one denotes $3d_{3/2}{}^3 3d_{5/2}$ component. The solid curve is the actual transition energy with the intermediate coupling scheme.

References

1. Kaufman, V. and Sugar, J., J. Phys. Chem. Ref. Data **15**, 321 (1986).
2. Wróblewski, D. *et al.*, Phys. Rev. Lett. **61**, 1724 (1988).
3. Isler, R. C. *et al.*, Phys. Plasmas **4**, 355 (1997).
4. Ida, K. and Hidekuma, S., Rev. Sci. Instrum. **60**, 867 (1989).
5. Feldman, U., Indelicato, P. and Sugar, J., J. Opt. Soc. Am. B **8**, 3 (1991).
6. Morgan, C. A. *et al.*, Phys. Rev. Lett. **74**, 1716 (1995).
7. Serpa, F. G. *et al.*, Phys. Rev. A **53**, 2220 (1996).
8. Porto, J. V., Kink, I. and Gillaspy, J. D., Phys. Rev. A **61**, 054501 (2000).
9. Bieber, D. J., Margolis, H. S., Oxley, P. K. and Silver, J. D., Physica Scripta **T73**, 64 (1997).
10. Utter, S. B., Beiersdorfer, P. and Brown, G. V., Phys. Rev. A **61**, 030503(R) (2000).
11. Träbert, E., Beiersdorfer, P., Utter, S. B. and Crespo López-Urrutia, J. R., Physica Scripta **58**, 599 (1998).
12. Beck, D. R., Phys. Rev. A **56**, 2428 (1997).
13. Beck, D. R., Phys. Rev. A **60**, 3304 (1999).
14. Currell, F. J., *et al.*, J. Phys. Soc. Jpn. **65**, 3186 (1996).
15. Parpia, F. A., Fischer, C. F. and Grant, I. P., Comput. Phys. Commun. **94**, 249 (1996).
16. Kato *et al.* in preparation.